

See discussions, stats, and author profiles for this publication at: <https://www.researchgate.net/publication/50890373>

Effects of Side-Chain Orientation on the Backbone Conformation of the Dehydrophenylalanine Residue. Theoretical and X-ray Study

ARTICLE *in* THE JOURNAL OF PHYSICAL CHEMISTRY B · MARCH 2011

Impact Factor: 3.3 · DOI: 10.1021/jp200949t · Source: PubMed

CITATIONS

10

READS

18

4 AUTHORS, INCLUDING:



Dawid Siodłak

Opole University

41 PUBLICATIONS 219 CITATIONS

[SEE PROFILE](#)



Małgorzata A Broda

Opole University

63 PUBLICATIONS 448 CITATIONS

[SEE PROFILE](#)

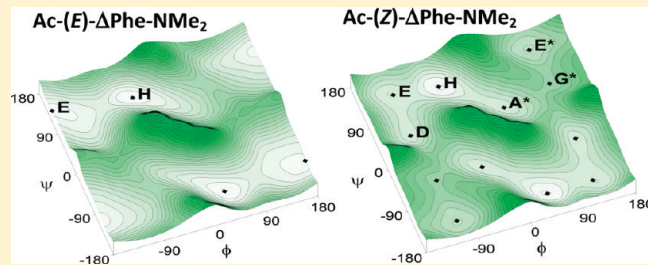
Effects of Side-Chain Orientation on the Backbone Conformation of the Dehydrophenylalanine Residue. Theoretical and X-ray Study

Aneta Buczek, Dawid Siodłak, Maciej Bujak, and Małgorzata A. Broda*

Faculty of Chemistry, University of Opole, Poland

Supporting Information

ABSTRACT: Two *E* isomers of α,β -dehydro-phenylalanine, Ac-(*E*)- Δ Phe-NHMe (**1a**) and Ac-(*E*)- Δ Phe-NMe₂ (**2a**), have been synthesized and their low temperature structures determined by single-crystal X-ray diffraction. A systematic theoretical analysis was performed on these molecules and their *Z* isomers (**1b** and **2b**). The ϕ,ψ potential energy surfaces were calculated at the MP2/6-31+G(d,p) and B3LYP/6-31+G(d,p) levels in the gas phase and at the B3LYP/6-31+G(d,p) level in the chloroform and water solutions with the SCRF-PCM method. All minima were fully optimized by the MP2 and DFT methods, and their relative stabilities were analyzed in terms of π -conjugation, internal H-bonds, and dipole–dipole interactions between carbonyl groups. The results indicate that all the studied compounds can adopt the conformation *H* ($\phi, \psi \approx \pm 40^\circ, \mp 120^\circ$) which is atypical for standard amino acids residues. A different arrangement of the side chain in the *E* and *Z* isomers causes them to have different conformational preferences. In the presence of a polar solvent both *Z* isomers of Δ Phe (**1b** and **2b**) are found to adopt the 3_{10} -helical conformation (left- and right-handed are equally likely). On the other hand, this conformation is not accessible or highly energetic for *E* isomers of Δ Phe (**1a** and **2a**). Those isomers have an intrinsic inclination to have an extended conformation. The conformational space of the *Z* isomers is much more restricted than that of the *E* derivative both in the gas phase and in solution. In the gas phase the *E* isomers of Δ Phe have lower energies than the *Z* ones, but in the aqueous solution the energy order is reversed.



INTRODUCTION

Conformationally restricted amino acids are widely used in the construction of peptide analogues with a controlled fold in the backbone. Among the α -amino acids whose structural rigidity can be used in the design of synthetic analogues of biologically important peptides with preferred secondary structures are α,β -didehydro- α -amino acids (in short: dehydroamino acids, Δ Xaa). Dehydroamino acids are nonstandard amino acids, with a double bond between the C^α and C^β atoms that constrains the side chain in the *E* or *Z* position. They have been found in nature in several peptides and enzymes, e.g., lantibiotics,^{1,2} tentoxin,³ microcystins, and nodularins.^{4–7} It has also been reported that they play a catalytic role in the active sites of some yeast⁸ and bacterial⁹ enzymes.

Dehydroamino acids are useful synthetic precursors for the synthesis of a number of unnatural amino acids and peptides.¹⁰ The enantioselective catalytic hydrogenation of *N*-acetyl dehydroamino acids is an efficient direct route to optically active α -amino acids.^{11,12} Dehydroamino acids can be used in the synthesis of β -pyrenyldehydroamino acids, a pyrenylalanine derivative, and heteroarylindoles with interesting antitumor activity in good-to-high yields.^{13,14} Incorporation of the (*Z*)- Δ Phe residue provides structural and proteolytic stability to the self-assembled peptide nanostructures.^{15,16} Dehydropeptides also show increased binding ability to metal ions.¹⁷ Some dehydroamino acids and corresponding peptides can function as radical scavengers, their reactive double bonds acting as a guard *in vitro* against oxidants.¹⁸

The presence of the $C^\alpha=C^\beta$ double bond generates unique conformational properties. The introduction of dehydroamino acid residues into bioactive peptide sequences has become a useful tool to study the structure–function relationship and to provide new analogues of enhanced activity (for reviews, see refs^{19–21}). Most of the studies of the conformational properties of dehydropeptides concern the *Z* isomer, because the majority of the preparative procedures predominantly or exclusively yield this isomer.²² On the other hand, both the *Z* and *E* forms occur in nature, and receptor proteins discriminate quite precisely between the two geometries of the side chains in their bioligands.^{23,24} It has been established that the configuration of the $C^\alpha=C^\beta$ double bond in the Δ Abu residue in phomalide is important for phototoxicity.²⁵ The affinities of the dehydropeptides containing (*E*)- Δ Phe toward cathepsin C are significantly higher than those determined for (*Z*)- Δ Phe-containing dehydropeptides.²⁶ Also theoretical studies confirm the different conformational properties of the *E* and *Z* isomers of dehydroamino acid residues.^{27–29}

The most studied dehydroamino acid residue to date has been dehydrophenylalanine of the *Z* configuration. A number of studies have clearly recognized the strong tendency of the (*Z*)- Δ Phe residue to stabilize both β -turns in short model peptides³⁰ and 3_{10}

Received: January 28, 2011

Revised: March 12, 2011

Published: March 28, 2011

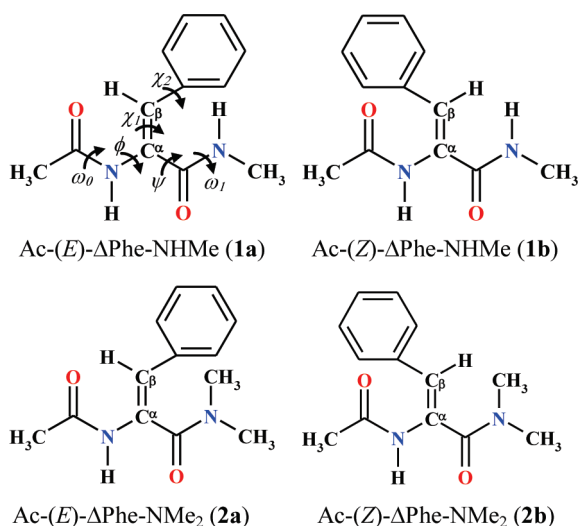


Figure 1. General formula and the definition of the selected torsion angles for the diamides studied in this work.

helical conformations in longer peptides or peptides with more than one dehydro residue³¹ both in solutions and in crystal structures. However, depending on the position and neighbors in the peptide chain, the (Z)-ΔPhe residue can also generate other secondary structural motifs.³² According to the limited literature data, (E)-ΔPhe in its crystal state adopts the conformation β ($\phi, \psi \sim -42^\circ, 124^\circ$) and the conformation α_L ($\phi, \psi \sim 51^\circ, 49^\circ$).^{33–35} In solution, the extended conformer C_S ($\phi, \psi \sim -179^\circ, 162^\circ$) can be also found.²⁹

N-Methylation is another structural modification of significant interest in the area of medicinal chemistry, because several compounds with good pharmacokinetic profiles are based on N-methylamino acid-containing substances.³⁶ N-Methylation is an important tool to modify lipophilicity, proteolytic stability, and bioavailability and to induce conformational rigidity to a peptide backbone. Short poly-N-methylated peptides or peptides containing alternating N-methylamide bonds and normal amide bonds have been especially successful as inhibitors of amyloidosis.³⁷ Despite the excessive interest in the biological activity of peptides containing N-methylamino acids, far less attention has been given to detailed structural investigations of such entities. Junctions of these two structural elements, a methylated N-terminal amide bond and dehydroamino acid, occur in natural peptides.^{38–44} N-Methylation of the C-terminal amide bond has considerable influence on the conformational properties of the dehydroamino acid residue, which can be useful in peptide design. Interestingly, the conformational space of the (Z)-ΔPhe residue is reduced, whereas the ΔAla residue is increased, as compared to non-methylated analogues.^{45,46}

The E isomer of the dehydrophenylalanine residue with a tertiary C-terminal amide bond has not been studied to date. Also the solvent effects on the conformational properties of dehydrophenylalanine residue were not taken into account in the up to date theoretical analysis. Moreover, it would be interesting to compare the conformational preferences of both the ΔPhe isomers since they have different well-defined side-chain orientations. Because side chains are directly involved in molecular recognition processes, their three-dimensional arrangement is crucial for adequate peptide–receptor interactions. Moreover, the peptide backbone conformation may be modulated, to a certain extent, by the side-chain orientation, and the two ΔPhe isomers are

excellent tools to investigate this effect because the aromatic substituent may interact with the peptide backbone not only sterically but also electronically through the aromatic π orbitals.

In the work reported here, a conformational study of E isomers of the ΔPhe residue combined with a secondary or tertiary amide bond at the C-terminal side have been undertaken. The DFT and MP2 calculations of both E and Z isomers (Figure 1) supported by the X-ray diffraction studies of the E isomers were performed. Calculations of the conformational properties were performed for the isolated molecules and in the polar environment of chloroform and water to mimic amino acids inside a folded protein or in aqueous solution, respectively. Hydrogen bonding interactions with solvent molecules influence the peptide conformations in solution, and also in the solid state where H-bonds between neighboring molecules become important. The aim of this article is to provide a comparison of the conformational properties of the E and Z isomers of the model dehydropeptides, Ac-ΔPhe-NHMe and Ac-ΔPhe-NMe₂, both in the gas phase and in a polar environment.

MATERIALS AND METHODS

Synthesis. Ac-ΔPhe-OH was obtained according to ref 47; Ac-(Z)-ΔPhe-NHMe and Ac-(Z)-ΔPhe-NMe₂ were obtained according to refs 48 and 49, respectively.

Benzophenone (5.46 g, 30 mM), Ac-(Z)-ΔPhe-NHMe (1.38 g, 6 mM), or Ac-(Z)-ΔPhe-NMe₂ (1.41 g, 6 mM) were dissolved in a solution of benzene (150 mL) and acetone (36 mL). The mixture was vigorously stirred using a magnetic stirrer at room temperature and irradiated using a UV lamp (254 nm) for 72 h. The reaction progress was monitored by HPLC analysis until the maximum E/Z ratio was obtained. The solvents were evaporated, and the remaining pale yellow oil was purified first by using flash column chromatography eluted by ethyl acetate to remove benzophenone.

The proper fractions of the E isomers were selected, the solvent was evaporated, and the remaining transparent oil was separated using the second flash column chromatography.⁵⁰ In both columns, silica gel 60 (0.040–0.063 mm) was used, and the fraction was checked on silica gel plates (TLC aluminum sheets, silica gel 60; Merck F254). Mixtures of acetone/hexane (40/60 v/v) and chloroform/ethanol (94/6 v/v) were applied as the eluents for Ac-(E)-ΔPhe-NHMe and Ac-(E)-ΔPhe-NMe₂, respectively.

Ac-(E)-ΔPhe-NHMe: yield 0.46 g (33%), purity 100% (HPLC), mp 130.58 °C (DSC), ¹H NMR (CDCl₃) δ: 2.2 (s, 3H, Ac), 2.7 (d, 3H, NMe), 5.9 (s, 1H, NH), 7.3 (m, SH, Ph), 7.9 (s, 1H, NH), 8.1 (s, 1H, CβH).

Ac-(E)-ΔPhe-NMe₂: yield 0.47 g (33%), purity 98% (HPLC), mp 144.46 °C (DSC), ¹H NMR (CDCl₃) δ: 2.1 (s, 3H, Ac), 2.7 and 2.9 (2s, 6H, NMe₂), 6.7 (s, 1H, CβH), 7.2 (m, SH, Ph), 8.5 (s, 1H, NH).

For X-ray diffraction measurements, Ac-(E)-ΔPhe-NMe₂ was dissolved in the MeOH/AcOEt mixture and crystallized using hexane as the antisolvent at lower temperature (7 °C), whereas Ac-(E)-ΔPhe-NMe was crystallized from ethyl acetate.

X-ray Crystal Structure Analysis. The low-temperature, at 85 K, diffraction data for Ac-(E)-ΔPhe-NHMe and Ac-(E)-ΔPhe-NMe₂·H₂O were collected on an Oxford Diffraction Xcalibur-1 diffractometer, with graphite monochromated Mo Kα ($\lambda = 0.71073$ Å) radiation, equipped with an Oxford Cryosystems cooler. The Oxford Diffraction CrysAlis CCD and CrysAlisPro programs were used during the data collection, cell refinement, and data

reduction processes.⁵¹ Both structures were solved by direct methods and refined, by a full-matrix least-squares method, on F^2 using SHELX-97.⁵² All non-H atoms were refined with anisotropic displacement parameters. All of the H-atoms were located in the subsequent difference Fourier maps and isotropically refined. The coordinates of the H-atoms attached to the N- and O-atoms were refined, whereas the refinement of H-atoms bound to the C-atoms was performed using a riding model. The isotropic displacement parameters of the H-atoms were taken with coefficients 1.5 and 1.2 times larger than the respective parameters of the methyl carbon/oxygen and the remaining carbon/nitrogen atoms, respectively. The structure drawings were prepared using Mercury.⁵³

Crystal Data for Ac-(E)-ΔPhe-NHMe. $C_{12}H_{14}N_2O_2$, $M = 218.25$, crystal size $0.38 \times 0.24 \times 0.13$ mm, orthorhombic, space group $Pna2_1$, $a = 7.0632(1)$, $b = 13.6350(3)$, $c = 12.1458(2)$ Å, $V = 1169.72(4)$ Å³, $\rho_{\text{calcd}} = 1.239$ g/cm³, $Z = 4$, $\mu = 0.086$ mm⁻¹, reflections collected 8934, $R_{\text{int}} = 0.0137$, data/parameters 1610/153, GOF on F^2 1.153, R_I (all data) = 0.0331, wR_2 (all data) = 0.0945.

Crystal Data for Ac-(E)-ΔPhe-NMe₂·H₂O. $C_{13}H_{16}N_2O_2 \cdot H_2O$, $M = 250.29$, crystal size $0.27 \times 0.25 \times 0.15$ mm, monoclinic, space group $P2_1/n$, $a = 11.4952(2)$, $b = 7.2281(1)$, $c = 16.0550(3)$ Å, $\beta = 94.246(2)$ °, $V = 1330.32(4)$ Å³, $\rho_{\text{calcd}} = 1.250$ g/cm³, $Z = 4$, $\mu = 0.089$ mm⁻¹, reflections collected 10347, $R_{\text{int}} = 0.0247$, data/parameters 3429/175, GOF on F^2 1.100, R_I (all data) = 0.0507, wR_2 (all data) = 0.1029.

The crystallographic data for Ac-(E)-ΔPhe-NHMe and Ac-(E)-ΔPhe-NMe₂·H₂O have been deposited at the Cambridge Crystallographic Data Centre as supplementary publication nos. CCDC 808030 and CCDC 808031, respectively. The data can be obtained free of charge via www.ccdc.cam.ac.uk/conts/retrieving.html (or from the Cambridge Crystallographic Data Centre, 12 Union Road, Cambridge CB2 1EZ, UK; fax: (+44) 1223 336033; e-mail: deposit@ccdc.cam.ac.uk).

Computational Procedures. The theoretical conformational properties of the *E* and *Z* isomers of the Ac-ΔPhe-NHMe (**1a**, **1b**) and Ac-ΔPhe-NMe₂ (**2a**, **2b**) diamides (Figure 1) were calculated using the Gaussian09 package.⁵⁴ Calculations were performed on molecules with the trans secondary amide groups ($\omega_0, \omega_1 \sim 180$ °). The ($\phi-\psi$) potential energy surfaces (PESs) of the studied molecules were calculated at the B3LYP/6-31+G(d,p)//B3LYP/6-31G(d)^{55,56} and the MP2/6-31+G(d,p)//B3LYP/6-31G(d) levels of theory with resolutions of 30° for the main-chain dihedral angles (ϕ and ψ). In each of the obtained structures, the geometrical parameters were fully relaxed, except for the constrained torsion angles ϕ and ψ . Because of the achiral nature of the studied molecules, only half of the maps were computed since $E(\phi, \psi) = E(-\phi, -\psi)$. To obtain an estimate of the solvation effects on the shape of the Ramachandran maps, single-point calculations were also conducted in each grid point using a self-consistent reaction field (SCRF) model. Specifically, we chose the polarizable continuum model (PCM) developed by Tomasi and co-workers to describe the bulk solvent.^{57,58} The energy surfaces were created using the Surfer 8 program.⁵⁹ Possible energy minima on the PES were investigated on every low-energy region of the map by full geometry optimization at the B3LYP/6-31+G(d,p) and MP2/6-31+G(d,p) levels in vacuo and by the B3LYP/6-31+G(d,p) method in chloroform and water using the PCM model. Frequency analyses were carried out to verify the nature of the minimum state of all the stationary points obtained and to calculate the zero-point vibrational energies (ZPVE), which were used to compute enthalpies

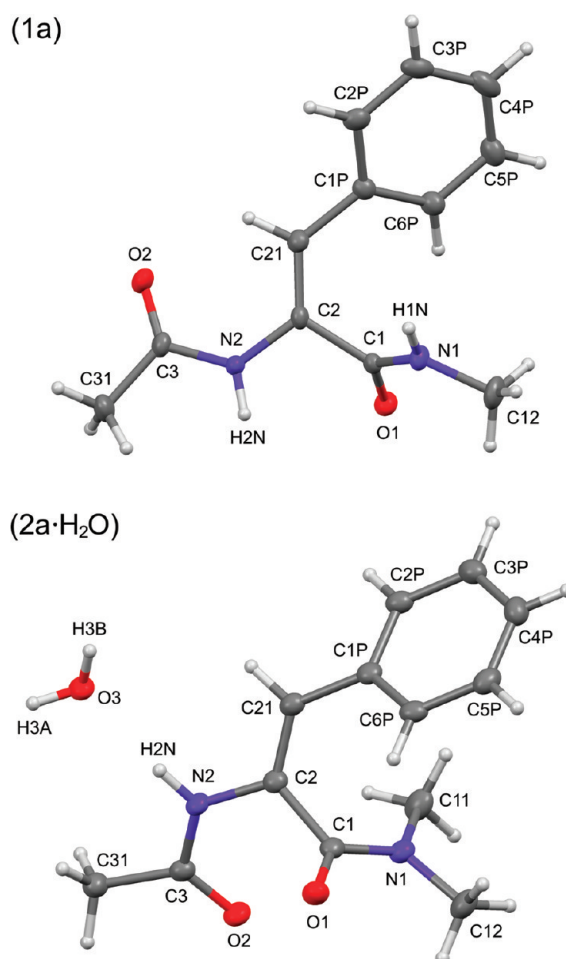


Figure 2. The solid-state molecular structures of Ac-(E)-ΔPhe-NHMe (**1a**) and Ac-(E)-ΔPhe-NMe₂·H₂O (**2a**·H₂O) showing the different molecular conformations and the atom-numbering scheme. Displacement ellipsoids are plotted at the 50% probability level.

and Gibbs free energies with scale factors of 0.98 and 0.96 at B3LYP and MP2 levels, respectively, at 25 °C and 1 atm.⁶⁰ As the overall conformational profiles of dehydropeptides can differ from those of common peptides, the energy-minimized conformers of the investigated molecules are described by a capital letter depending on the values of ϕ and ψ for the backbone.⁶¹ Conformations *E*, *E**, *H*, *A*, *A**, *D*, and *G** are equivalent to the extended (C_S), α_D , polyproline-like (β or P_{II}), α -helical (α_R and α_L), β_2 , and α' structures in the literature, respectively. (Comparison of these two methods for labeling backbone conformers of amino acid diamides according to their locations on a Ramachandran map is given in Figure S1, Supporting Information.)

RESULTS AND DISCUSSION

X-ray Crystal Structures: Adopted Conformations and Association Patterns. The molecular structures of Ac-(E)-ΔPhe-NHMe and Ac-(E)-ΔPhe-NMe₂·H₂O are depicted in Figure 2, and their selected geometric parameters are compared with those for *Z* isomers (**1b** and **2b**) in Table S1 (Supporting Information). Most of the molecular dimensions of the studied compounds are, in principle, comparable and consistent with those obtained from other studies of related compounds.^{62,63}

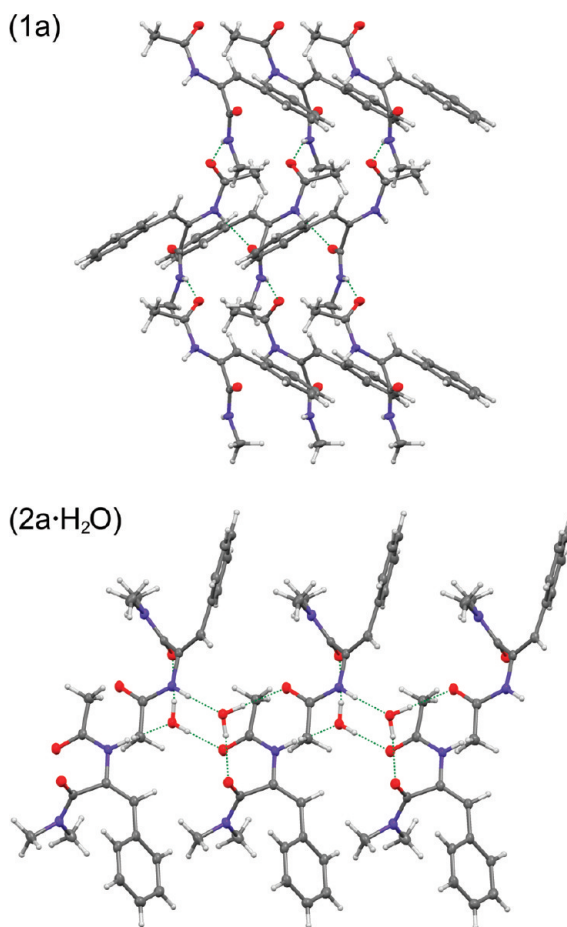


Figure 3. The association patterns of $\text{Ac}-(\text{E})\text{-}\Delta\text{Phe-NHMe}$ (**1a**) and $\text{Ac}-(\text{E})\text{-}\Delta\text{Phe-NMe}_2 \cdot \text{H}_2\text{O}$ (**2a**· H_2O) molecules in their crystal structures. The dotted lines indicate the $\text{N}-\text{H}\cdots\text{O}$ and $\text{O}-\text{H}\cdots\text{O}$ hydrogen bonds. Displacement ellipsoids are plotted at the 50% probability level.

However, some differences, mainly associated with different intra- and intermolecular interactions, could be found. The compounds clearly show different conformational preferences. The ϕ and ψ torsion angles for $\text{Ac}-(\text{E})\text{-}\Delta\text{Phe-NHMe}$ are $-163.46(16)^\circ$ and $-116.19(17)^\circ$, whereas angles of $-36.23(14)^\circ$ and $124.08(10)^\circ$ were found for $\text{Ac}-(\text{E})\text{-}\Delta\text{Phe-NMe}_2 \cdot \text{H}_2\text{O}$. In both cases, the opposite $-\phi$ and $-\psi$ angles of $163.46(16)^\circ$ and $116.19(17)^\circ$ as well as $36.23(14)^\circ$ and $-124.08(10)^\circ$, respectively, were found for the corresponding symmetry-related molecules presented in the crystal structures.

The $\text{N}2-\text{C}2-\text{C}1$ angle is $5.31(17)^\circ$ smaller for $\text{Ac}-(\text{E})\text{-}\Delta\text{Phe-NHMe}$ than for $\text{Ac}-(\text{E})\text{-}\Delta\text{Phe-NMe}_2 \cdot \text{H}_2\text{O}$, which confirms the presence of an intramolecular $\text{N}2-\text{H}2\text{N}\cdots\text{O}1$ C_5 -type interaction with an $\text{N}2\cdots\text{O}1$ distance of $2.934(2)$ Å and an $\text{N}2-\text{H}2\text{N}\cdots\text{O}1$ angle of $91(2)^\circ$ in the former compound. Further, the spatial arrangement of the N-terminal amide group, in $\text{Ac}-(\text{E})\text{-}\Delta\text{Phe-NHMe}$, enables the internal $\text{C}21-\text{H}21\cdots\text{O}2$ interaction (Table S2 in Supporting Information). The ϕ torsion angle, which is close to 180° in $\text{Ac}-(\text{E})\text{-}\Delta\text{Phe-NHMe}$, may indicate an π -electron conjugation between the N-terminal amide group and the double $\text{C}2=\text{C}21$ bond. However, all of these intramolecular interactions are exclusively characteristic for $\text{Ac}-(\text{E})\text{-}\Delta\text{Phe-NHMe}$. The weaker $\text{N}2\cdots\text{O}1$ interaction with a distance of $2.992(1)$ Å was found in the structure of $\text{Ac}-(\text{E})\text{-}\Delta\text{Phe-NMe}_2 \cdot \text{H}_2\text{O}$, too. $\text{Ac}-(\text{E})\text{-}\Delta\text{Phe-NMe}_2 \cdot \text{H}_2\text{O}$ also shows a pair

of intramolecular $\text{O}\cdots\text{C}$ interactions, $\text{O}2\cdots\text{C}1$ ($2.700(1)$ Å) and $\text{O}1\cdots\text{C}3$, with a somewhat longer separation distance of $3.316(1)$ Å, arranged in a slightly sheared antiparallel motif.⁶⁴ The $\text{C}3-\text{O}2$ bond of the N-terminal amide group for $\text{Ac}-(\text{E})\text{-}\Delta\text{Phe-NMe}_2 \cdot \text{H}_2\text{O}$ is longer, by $0.015(2)$ Å, than that for $\text{Ac}-(\text{E})\text{-}\Delta\text{Phe-NHMe}$, which is due to the $\text{O}3-\text{H}3\text{B}\cdots\text{O}2$ hydrogen bond between the $\text{Ac}-(\text{E})\text{-}\Delta\text{Phe-NMe}_2$ and H_2O molecules. The $\text{C}6\text{P}-\text{C}1\text{P}-\text{C}21-\text{C}2$ torsion angles of $31.4(3)^\circ$ and $-39.95(16)^\circ$ for $\text{Ac}-(\text{E})\text{-}\Delta\text{Phe-NHMe}$ and $\text{Ac}-(\text{E})\text{-}\Delta\text{Phe-NMe}_2 \cdot \text{H}_2\text{O}$, respectively, indicate that in both molecules, a possible π -electron conjugation between the phenyl rings and the double $\text{C}2=\text{C}21$ bonds cannot be realized.

Figure 3 shows the association patterns of both $\text{Ac}-(\text{E})\text{-}\Delta\text{Phe-NHMe}$ and $\text{Ac}-(\text{E})\text{-}\Delta\text{Phe-NMe}_2 \cdot \text{H}_2\text{O}$ molecules in their crystal structures. The main forces responsible for the molecular associations are the $\text{N}-\text{H}\cdots\text{O}$ and $\text{O}-\text{H}\cdots\text{O}$ hydrogen bonds. In the structure of $\text{Ac}-(\text{E})\text{-}\Delta\text{Phe-NHMe}$ (**1a**) each molecule is involved in four $\text{N}-\text{H}\cdots\text{O}$ hydrogen bonds by means of its amide groups with four neighboring molecules (Figure 3). The N-terminal amide groups interact with the C-terminal amide groups, and in turn, the C-terminal amide groups are hydrogen bonded to the N-terminal amide groups of the neighboring molecules. Therefore, each molecule forms the $\text{N}-\text{H}\cdots\text{O}$ hydrogen bonds by joining the N-terminal $\text{N}-\text{H}$ and C-terminal C=O groups to the enantiomeric molecules, and the N-terminal C=O and C-terminal $\text{N}-\text{H}$ groups to the homomeric molecules. Thus, $\text{Ac}-(\text{E})\text{-}\Delta\text{Phe-NHMe}$ reveals a complicated three-dimensional association pattern.

$\text{Ac}-(\text{E})\text{-}\Delta\text{Phe-NMe}_2 \cdot \text{H}_2\text{O}$ (**2a**· H_2O) shows a different association behavior that is mainly determined by the presence of the ‘additional’ water molecules in its crystal structure (Figure 3). The hydrogen bond $\text{N}-\text{H}\cdots\text{O}$ and $\text{O}-\text{H}\cdots\text{O}$ interactions are the main forces causing the molecular association. Each $\text{Ac}-(\text{E})\text{-}\Delta\text{Phe-NMe}_2$ molecule is joined to three H_2O molecules, and at the same time, each H_2O molecule is connected with three $\text{Ac}-(\text{E})\text{-}\Delta\text{Phe-NMe}_2$ molecules. The N-terminal amide group interacts with two water molecules, creating a molecular chain of alternating $\text{Ac}-(\text{E})\text{-}\Delta\text{Phe-NMe}_2$ and H_2O molecules, connected by the alternating $\text{N}-\text{H}\cdots\text{O}$ and $\text{O}-\text{H}\cdots\text{O}$ hydrogen bonds. The C-terminal amide group is involved in the $\text{O}-\text{H}\cdots\text{O}$ hydrogen bond with the third water molecule of the parallel $\text{Ac}-(\text{E})\text{-}\Delta\text{Phe-NMe}_2$ and H_2O molecular chain. In consequence, a double chain, built of homomeric $\text{Ac}-(\text{E})\text{-}\Delta\text{Phe-NMe}_2$ and H_2O molecules, is formed. The second $\text{Ac}-(\text{E})\text{-}\Delta\text{Phe-NMe}_2$ enantiomeric forms together with H_2O molecules create the same arrangement. The phenyl rings of $\text{Ac}-(\text{E})\text{-}\Delta\text{Phe-NMe}_2$ molecules are located on the opposite sides of the molecular chains.

Theoretical Conformational Analysis. The $E = f(\phi, \psi)$ potential energy surfaces (PES) of the studied diamides $\text{Ac}-\Delta\text{Phe-NHMe}$ (**1a**, **1b**) and $\text{Ac}-\Delta\text{Phe-NMe}_2$ (**2a**, **2b**) calculated in vacuo (gas phase), in chloroform, and in an aqueous environment are shown in Figures 4 and 5, respectively. Tables 1 and 2 list the relative energies, thermodynamic properties, and selected torsion angles of local minima from the upper halves of the maps of **1a**, **1b** and **2a**, **2b**, respectively.

The folding and stability of polypeptide chains are due to many different and simultaneous noncovalent interactions. The analysis of the stabilizing forces in the studied dehydroamino acids derivatives was performed on the assumption that the internal $\text{X}-\text{H}\cdots\text{A}$ hydrogen bonds and, among the dipole–dipole attractions, those between the carbonyl groups determine their conformational preferences.^{65,64} Tables S3 and S4 (Supporting

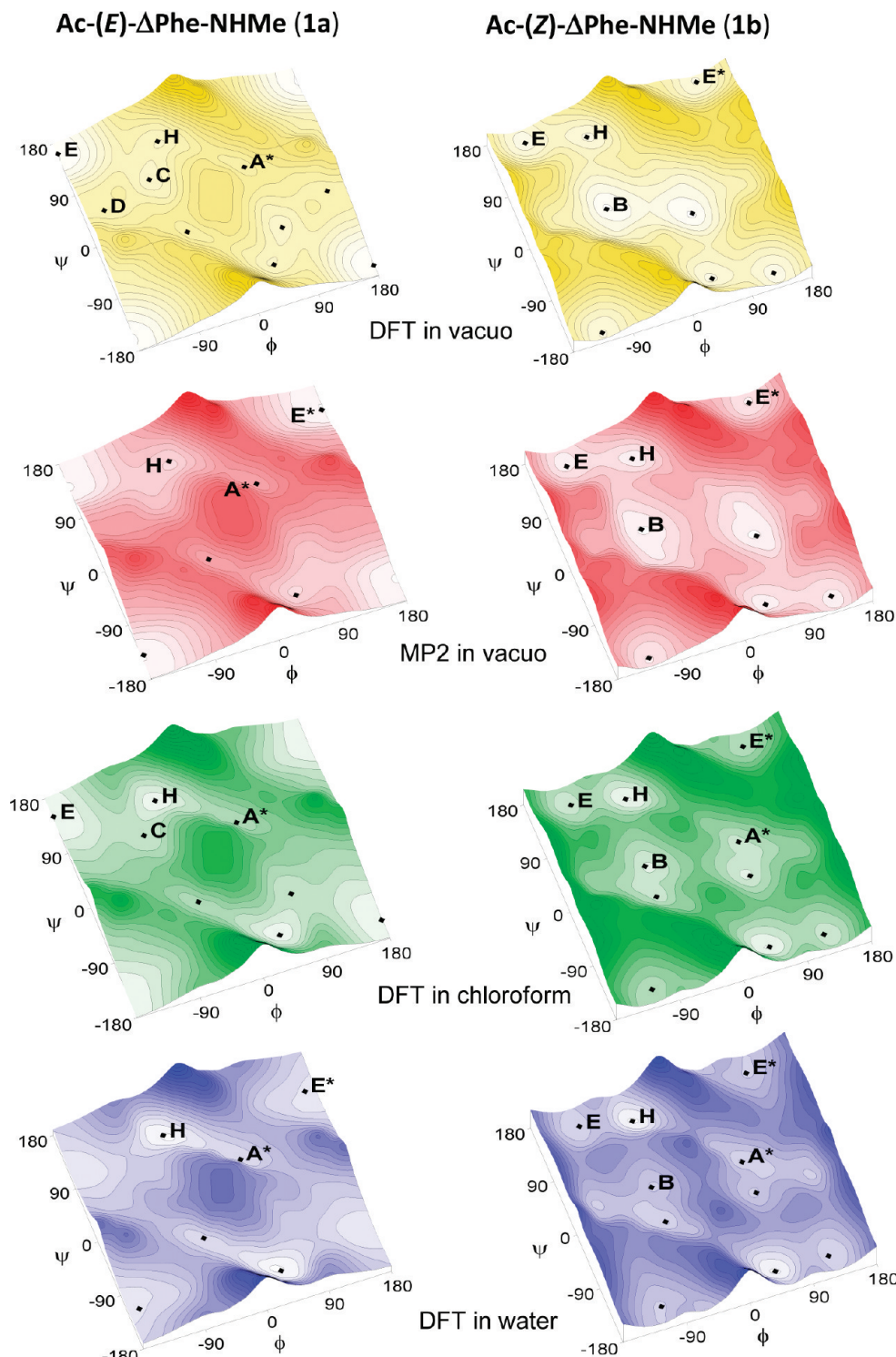


Figure 4. The potential energy surfaces $E = f(\phi, \psi)$ of $\text{Ac}-(E)\text{-}\Delta\text{Phe-NHMe}$ (**1a**) and $\text{Ac}-(Z)\text{-}\Delta\text{Phe-NHMe}$ (**1b**) in vacuo calculated by the B3LYP/6-31+G(d,p) and by the MP2/6-31+G(d,p) methods, and in chloroform and in water calculated by the B3LYP/6-31+G(d,p) method. Energy contours are drawn every 1 kcal/mol. Local minima are represented by ◆, and minima found on the upper halves of the maps are described by the general shorthand letter notation.

Information) collect the geometric parameters of all intramolecular hydrogen bonds which are stabilizing conformers of **1** and **2**, respectively. The geometrical characteristics of carbonyl dipole–dipole interactions are given in Table S5 (Supporting Information). The interactions stabilizing the conformers of **1a**, **1b**, and **2b**, obtained by B3LYP/6-31+G^{**} in the gas phase,

were analyzed previously^{29,46} but are repeated here for comparison. The structures of $\text{Ac}-(E)\text{-}\Delta\text{Phe-NMe}_2$ (**2a**) conformers are compared with the corresponding two main conformers of $\text{Ac}-(Z)\text{-}\Delta\text{Phe-NMe}_2$ (**2b**) and are depicted in Figure 6. (All conformers of **2b** are shown in Figure S2 in Supporting Information).

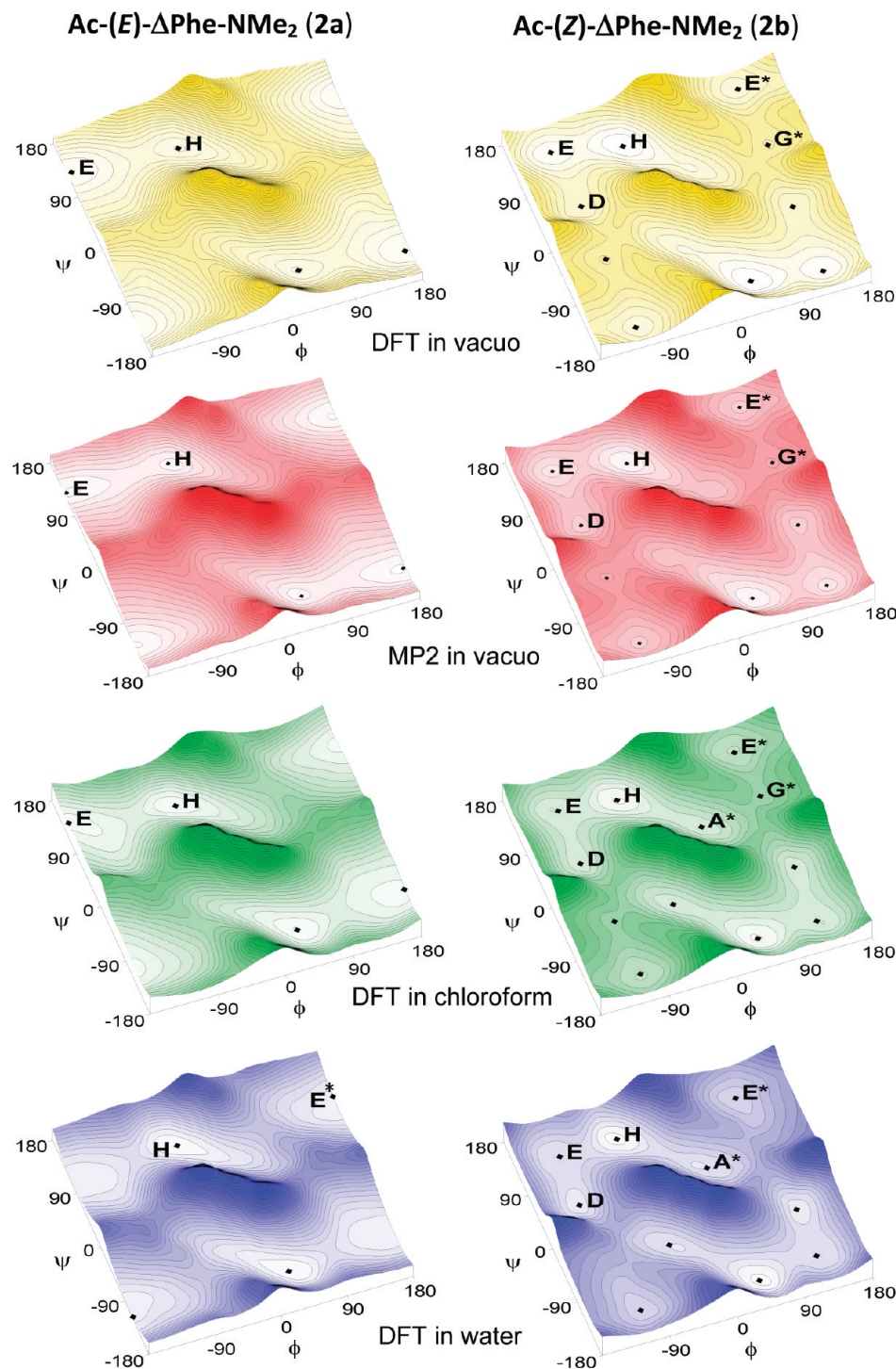


Figure 5. The potential energy surfaces $E = f(\phi, \psi)$ of $\text{Ac}-(E)\text{-}\Delta\text{Phe-NMe}_2$ (**2a**) and $\text{Ac}-(Z)\text{-}\Delta\text{Phe-NMe}_2$ (**2b**) in vacuo calculated by the B3LYP/6-31+G(d,p) and by the MP2/6-31+G(d,p) methods, and in chloroform and in water calculated by the B3LYP/6-31+G(d,p) method. Energy contours are drawn every 1 kcal/mol. Local minima are represented by \blacklozenge , and minima found on the upper halves of the maps are described by the general shorthand letter notation.

$\text{Ac}-(E)\text{-}\Delta\text{Phe-NHMe}$ (1a**).** Figure 4 shows the 3D-Ramachandran map for the **1a** molecule calculated by DFT method in the gas phase. The shape of this surface is almost identical to those obtained earlier²⁹ at the B3LYP/6-31G*//HF/3-21G level, but in this case we localized additional, high energy helical conformers A ($\phi, \psi = -56^\circ, -36^\circ$) and A^* ($\phi, \psi = 56^\circ, 36^\circ$). The PES of **1a** calculated by the MP2 method reveals only three minima

and their mirror images (including the helical ones) and predicts a visibly smaller difference in energy between the two lowest conformers, compared to the DFT results. This can be attributed to the change in the backbone angle ψ in conformer E, from 162° at the DFT level to 142° in MP2, which causes a worsening of the geometry of all the H-bonds stabilizing this conformer (Table S3) as well as π -conjugation and causing an increase in the

Table 1. Selected Torsion Angles (deg) and Thermodynamic Properties (kcal/mol) of Local Minima for 1a, 1b Isomers of Ac- Δ Phe-NHMe

conformer	B3LYP/6-31+G** in the Gas Phase					
	ϕ	ψ	χ_2	ΔE	ΔH	ΔG
Ac-(E)- Δ Phe-NHMe (1a)						
E (C _S)	-178.6	162.3	-55.5	0.00	0.00	0.00
H (β)	-43.2	123.1	-31.2	4.37	4.57	4.33
C (C ₇)	-74.6	68.8	-24.4	4.23	4.23	4.35
D ($\beta 2$)	-154.0	38.7	-24.6	6.66	6.66	6.29
A* (α_L)	55.7	36.3	-18.7	7.26	7.32	7.06
Ac-(Z)- Δ Phe-NHMe (1b)						
B (C ₇)	-55.8	24.4	-32.8	1.20	0.99	2.02
H (β)	-43.8	138.8	-28.7	2.47	2.52	2.87
E (C _S)	-129.1	159.8	19.0	2.52	2.51	2.90
E* (α_D)	132.6	170.3	-21.3	2.74	2.75	3.12
MP2/6-31+G** in the Gas Phase						
conformer	ϕ	ψ	χ_2	ΔE	ΔH	ΔG
Ac-(E)- Δ Phe-NHMe (1a)						
E* (C _S)	176.6	141.5	-51.4	0.00	0.00	0.00
H (β)	-42.9	128.0	-41.0	2.46	2.66	2.45
A* (α_L)	50.3	44.9	-51.3	7.14	7.29	6.66
Ac-(Z)- Δ Phe-NHMe (1b)						
B (C ₇)	-69.5	31.5	-47.9	1.24	1.20	1.26
H (β)	-44.3	138.4	-43.5	1.54	1.64	1.61
E (C _S)	-130.5	156.4	43.2	1.53	1.57	1.62
E* (α_D)	130.6	166.0	-38.5	1.77	1.81	1.90
B3LYP/6-31+G** in Chloroform						
conformer	ϕ	ψ	χ_2	ΔE	ΔH	ΔG
Ac-(E)- Δ Phe-NHMe (1a)						
E (C _S)	-177.8	153.1	-47.8	0.00	0.01	0.00
H (β)	-42.5	127.5	-32.4	2.04	2.19	2.14
C (C ₇)	-76.2	70.1	-18.0	3.27	3.26	3.33
A* (α_L)	50.4	43.2	27.1	4.32	4.41	4.23
Ac-(Z)- Δ Phe-NHMe (1b)						
H (β)	-45.9	141.9	-27.6	0.04	0.01	0.63
B (C ₇)	-60.1	25.7	-27.6	0.17	0.00	0.80
A* (α_L)	66.5	17.6	25.2	0.20	0.27	1.12
E (C _S)	-128.0	156.5	19.2	0.85	0.86	1.21
E* (α_D)	129.4	165.2	-20.7	1.27	1.27	1.69
B3LYP/6-31+G** in Water						
conformer	ϕ	ψ	χ_2	ΔE	ΔH	ΔG
Ac-(E)- Δ Phe-NHMe (1a)						
E (C _S)	177.6	147.0	-44.2	1.61	1.72	0.77
H (β)	-40.6	127.5	-32.0	2.49	2.57	2.53
A* (α_L)	49.3	45.3	31.2	3.25	3.38	2.90
Ac-(Z)- Δ Phe-NHMe (1b)						
A* (α_L)	67.4	18.9	17.9	0.00	0.00	0.00
H (β)	-46.7	142.4	-26.8	0.16	0.19	0.20
B (C ₇)	-61.8	25.8	-24.7	1.28	1.17	1.38
E* (α_D)	125.3	160.2	-20.8	1.71	1.79	1.41
E (C _S)	-128.2	156.0	20.0	1.55	1.58	1.50

Table 2. Selected Torsion Angles (deg) and Thermodynamic Properties (kcal/mol) of Local Minima for 2a, 2b Isomers of Ac- Δ Phe-NMe₂

conformer	B3LYP/6-31+G** in the Gas Phase					
	ϕ	ψ	χ_2	ΔE	ΔH	ΔG
Ac-(E)- Δ Phe-NMe ₂ (2a)						
E (C _S)	-174.2	129.8	-36.4	0.00	0.00	0.00
H (β)	-37.6	116.4	-30.9	1.69	1.47	1.47
Ac-(Z)- Δ Phe-NMe ₂ (2b)						
H (β)	-38.6	127.7	-31.1	0.56	0.37	0.11
E (C _S)	-127.7	146.4	15.8	1.69	1.70	1.43
D ($\beta 2$)	-124.1	45.3	22.4	4.76	3.90	3.83
E* (α_D)	124.5	155.5	-20.2	3.93	4.59	4.26
G* (α')	125.9	50.4	-18.6	7.41	7.28	6.75
MP2/6-31+G** in the Gas Phase						
conformer	ϕ	ψ	χ_2	ΔE	ΔH	ΔG
Ac-(E)- Δ Phe-NMe ₂ (2a)						
E (C _S)	-177.6	128.6	-41.5	0.00	0.00	0.36
H (β)	-42.4	127.2	-41.7	0.57	0.32	0.00
Ac-(Z)- Δ Phe-NMe ₂ (2b)						
H (β)	-37.3	127.2	-41.8	1.22	1.06	1.50
E (C _S)	-130.3	143.4	43.5	2.56	2.48	2.70
D ($\beta 2$)	-127.5	46.0	47.1	4.17	3.90	4.20
E* (α_D)	122.9	154.1	-34.8	4.67	4.52	4.58
G* (α')	128.7	50.0	-36.2	7.76	7.44	7.58
B3LYP/6-31+G** in Chloroform						
conformer	ϕ	ψ	χ_2	ΔE	ΔH	ΔG
Ac-(E)- Δ Phe-NMe ₂ (2a)						
H (β)	-35.7	117.8	-30.1	1.25	1.20	1.53
E (C _S)	-174.7	125.3	-36.0	0.81	0.92	1.59
Ac-(Z)- Δ Phe-NMe ₂ (2b)						
H (β)	-40.4	131.1	-29.9	0.00	0.00	0.00
E (C _S)	-128.9	143.8	17.6	1.59	1.73	2.49
A* (α_L)	30.5	57.2	35.4	1.84	1.85	2.07
E* (α_D)	118.1	147.9	-18.9	3.49	3.60	3.92
D ($\beta 2$)	-125.2	47.0	22.0	3.53	3.55	3.91
G* (α')	120.3	58.1	-17.6	5.78	5.75	5.87
B3LYP/6-31+G** in Water						
conformer	ϕ	ψ	χ_2	ΔE	ΔH	ΔG
Ac-(E)- Δ Phe-NMe ₂ (2a)						
H (β)	-33.7	117.4	-29.2	1.26	1.20	1.10
E* (C _S)	179.8	120.0	-34.6	1.70	1.71	0.52
Ac-(Z)- Δ Phe-NMe ₂ (2b)						
H (β)	-41.7	133.1	-28.6	0.00	0.00	0.00
A* (α_L)	37.3	52.8	30.7	0.95	0.98	1.04
E (C _S)	-129.9	142.5	18.7	1.94	2.02	2.19
E* (α_D)	112.8	141.1	-20.1	2.88	2.95	2.89
D ($\beta 2$)	-126.7	46.3	22.7	3.14	3.14	3.28

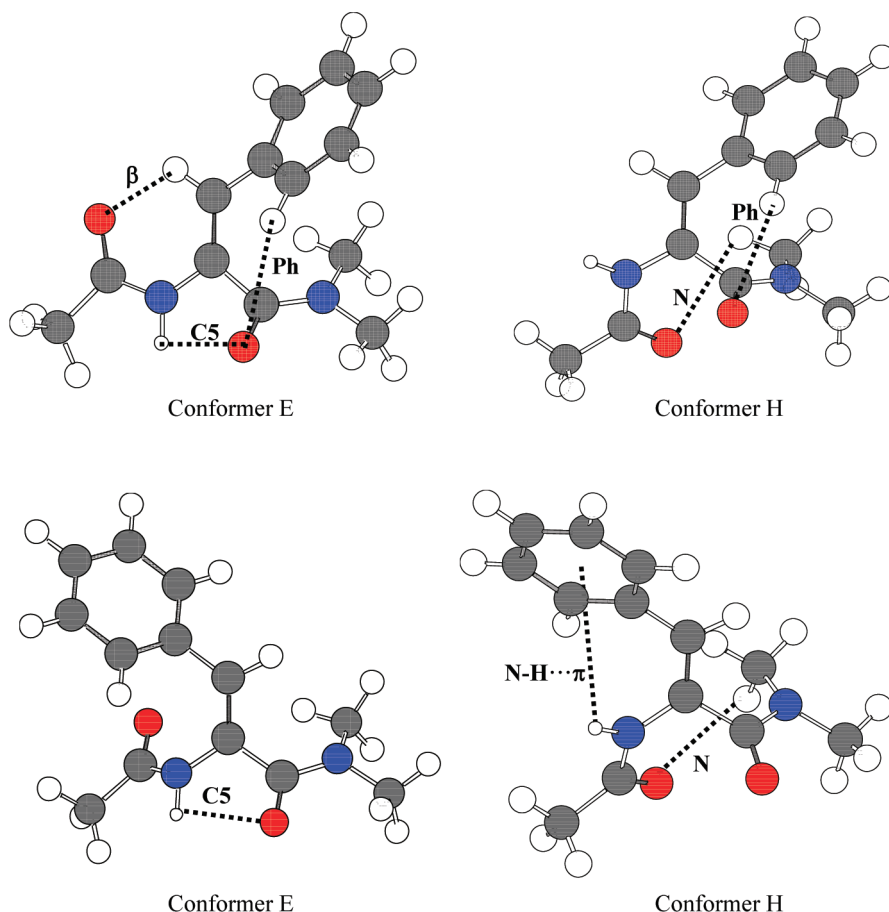


Figure 6. The E and H conformers of $\text{Ac}-(E)\text{-}\Delta\text{Phe-NMe}_2$ (**2a**) and $\text{Ac}-(Z)\text{-}\Delta\text{Phe-NMe}_2$ (**2b**) optimized at the MP2/6-31+G(d,p) level in the gas phase. Hydrogen bonds are represented by dotted lines.

conformer energy. The DFT results indicate that increasing the solvent polarity causes a reduction in the number of conformers, from five conformers in the gas phase, and four in the chloroform, to three in the water. In all the studied environments the extended conformer E (C_5) is the lowest in energy, the second is conformer H, and the last is the helical conformer A^* , but the differences between the conformers' energies diminish with an increase in solvent polarity. On going from the gas phase to chloroform and water, the largest shift in the backbone torsion angle is observed for the angle ψ (by -15°) in conformer E, which decreases the energy of all the intramolecular hydrogen bonds stabilizing this conformation (Table S3) and makes the π -electron conjugation on the C-terminus negligible. On the other hand, this change causes exposure to the solvent polar groups of the molecule and a greater opportunity for stronger intermolecular H-bonds.

$\text{Ac}-(Z)\text{-}\Delta\text{Phe-NHMe}$ (1b**).** The potential energy surfaces of the **1b** molecule in the gas phase were already calculated by the molecular mechanics,²⁷ ab initio,⁴⁶ and DFT/B3LYP methods.²⁹ The Ramachandran maps of the **1b** diamide in the gas phase calculated in this work by DFT and MP2 methods are very similar (Figure 4). Both maps show four local minima and their mirror images. The most preferred conformation is calculated to be the B structure mainly stabilized by a short $C_7\text{N}1-\text{H}\cdots\text{O}2$ hydrogen bond. However, so far in theoretical studies, the impact of the solvent on the shape of the PES surface was neglected. The solvent environment considerably influences the conformational

properties of the *Z* isomer of the ΔPhe derivative, and maps of **1b** in chloroform and water reveal additional, both right- and left-handed, helical local minima A ($\phi, \psi = -67^\circ, -18^\circ$) and A^* ($\phi, \psi = 67^\circ, 18^\circ$) with ϕ, ψ values typical for 3_{10} helix. Moreover, this conformer becomes the global minimum of $\text{Ac-}\Delta\text{Phe-NHMe}$ in a water environment.

$\text{Ac}-(E)\text{-}\Delta\text{Phe-NMe}_2$ (2a**).** The 3-D PESs of the **2a** diamide calculated by the DFT and MP2 methods in the gas phase are shown in Figure 5. These conformational maps reveal only two minima and their mirror counterparts. Although the overall shapes of the PESs obtained by these two methods are very similar, closer inspection reveals some minor differences in the predicted properties of the located minima. The thermodynamic properties calculated by B3LYP indicate that the extended conformer E ($\phi, \psi = -174^\circ, 130^\circ$) is more stable and its free energy (ΔG) is about 1.5 kcal/mol lower than the free energy of the second conformer H ($\phi, \psi = -38^\circ, 116^\circ$). The difference between the enthalpies of these two conformers is also 1.5 kcal/mol and between the electronic energies (ΔE_e) is slightly higher (1.7 kcal/mol). On the other hand, the free energies, as calculated by MP2, for these two conformers of molecule **2a** are almost equal. The MP2 geometry of the conformer E ($\phi, \psi = -178^\circ, 129^\circ$) is very similar to those obtained by B3LYP, but the conformer H ($\phi, \psi = -42^\circ, 127^\circ$) is, regarding the ψ angle, distinctly more extended. The shifts in the backbone torsion angles ϕ, ψ are 5° and 11° , respectively. The stability of conformer E can be ascribed to the N-terminal π -electron conjugation and the three hydrogen

bonds (Figure 6, Table S4). The first one closes the five-member ring (C_5): H-bond $N2-H \cdots O1$, and the next two are interactions of C–H groups of the side chain with the oxygen atoms of the carbonyl groups: $C^\delta-H \cdots O1$ and a very short $C^\beta-H \cdots O2$. The latter one closes the hexagonal (C_6) ring and has a similar geometry to the analogous $C^\beta-H \cdots O$ bonds found in the Δ Ala residue by X-ray diffraction⁶⁶ and in the Δ Ala and (*E*)- Δ Phe derivatives characterized by theoretical calculations.²⁹ The second conformer H has only two rather long C–H \cdots O H-bonds. So its presence on the PES with an energy comparable to conformer E can be explained by internal stabilization from a relatively short and strong dipole attraction between the carbonyls of the amide bonds (Table S5).

In water, the overall shape of the conformational map of **2a** is similar to those in the gas phase, except that the energy and enthalpy of minimum H are lower than those of minimum E, but in the free energies of these two conformers the order is reversed (Table 2). On going from the gas phase to water, there are some shifts in the backbone torsion angles ϕ and ψ for both conformers. The calculated shifts are larger for conformer E ($\phi, \psi = 180^\circ, 120^\circ$): 6° in ϕ and 10° in ψ . This is associated with a small increase in distance between the $H2N$ and $O1$ atoms (from 2.3 Å in the gas phase to 2.5 Å in the water) and a worsening of the other geometrical parameters of the $N2-H \cdots O1$ hydrogen bond. As a result, the $N2-H$ and $C1=O1$ groups become more exposed to the solvent. The values of the ϕ, ψ angles indicate that the N-terminal π -electron conjugation influences the stability of the conformer while the C-terminal π -electron conjugation should not be considered. The water-induced changes in the geometry of the conformer H ($\phi, \psi = -33^\circ, 118^\circ$) are smaller, only 4° in ϕ and ψ , but these changes are sufficient to break the $C(N)-H \cdots O2$ hydrogen bond.

Ac-(Z)- Δ Phe-NMe₂ (**2b**). The conformational maps for the Z isomer **2b**, calculated by the DFT and MP2 methods in the gas phase, are shown in Figure 5. The overall shapes of these maps are quite similar to those at the HF/6-31G*/HF/3-21G level published previously.⁴⁶ Both maps reveal five local minima with the conformational stabilities in the same order H > E > D > E* > G*, calculated by ΔG . The positions of the minima found by these two methods are also very similar. The largest difference in the backbone torsion angle is only 3.4° and is observed for the ϕ of conformer D. The most preferred conformation of **2b** is calculated to be H at both levels in the gas phase, but according to the B3LYP results, its free energy is almost the same as the free energy of conformer E of the *E*-isomer (**2a**), while at the MP2 level it has 1.5 kcal/mol higher free energy despite the fact that the torsion angles ϕ, ψ of conformer H of **2b**, calculated by both methods, are very similar. The structure of conformer H ($\phi, \psi = -37^\circ, 127^\circ$) is stabilized by $N2-H \cdots \pi$ and $C-H \cdots O2$ hydrogen bonds and additionally by carbonyl–carbonyl interaction with almost the same geometry as that in conformer H of the *E*-isomer (**2a**). The second preferred conformer is E with only 1.2 kcal/mol higher free energy than conformer H and a C_5 hydrogen bond $N2-H \cdots O1$. The phenyl ring in the Z position imposes steric constraints on the N-terminus in an extended conformation of **2b** and causes a reduction in the torsion angle ϕ from -178° in conformer E of **2a** to -130° in conformer E of **2b**. This decreases the π -electron conjugation between the N-terminal amide bond and the α,β -double bond, which causes an increase in free energy of the conformer of about 2.3 kcal/mol even though the geometry of the C_5 hydrogen bonds in both conformers have almost identical geometrical parameters. The

remaining conformers have distinctly higher energies ($\Delta E > 3$ kcal/mol) and are practically unavailable for the molecule.

The solvent effect on the conformational properties of **2b** is slightly larger than in the case of isomer **2a**. Although the overall shape of the conformational map for **2b** in water is similar to the one in the gas phase, the new local minimum A* ($\phi, \psi = 37^\circ, 53^\circ$) corresponding to the helical structure appears on the PES while the highest in energy minimum G* disappears. Interaction with the water environment diminishes the free energy gap between the conformers of **2b**, which are lowest and highest in energy, from 6.64 kcal/mol (6.08 kcal/mol at MP2 level) in the gas phase to 3.28 kcal/mol in the water. In fact, in the water phase, conformer H becomes a global minimum of the compound, but its energy is only about 1 kcal/mol lower than the energy of conformer A*. On going from the gas phase to the water phase, the shifts in torsion angles ϕ and ψ are for conformer H, $+3^\circ$ and $+5^\circ$, respectively, which cause the breaking of the $C(N)-H \cdots O2$ hydrogen bond, but the $N-H \cdots \pi$ and dipole–dipole interactions are retained in water with almost the same geometry as in the gas phase. Conformer A* is stabilized by the $N-H \cdots \pi$ and $C-H \cdots O$ hydrogen bonds as well as by dipole attraction between the carbonyls of the amide bonds. Note that the gap in energy between the conformers lowest and highest in energy is smaller for **2a** than for **2b**, in opposition to **1a** and **1b** analogues.

Comparison of Theoretical and X-ray Results. Figure 7 presents the distribution of the solid-state conformations of the dehydrophenylalanine residues retrieved from The Cambridge Structural Database (CSD),⁶⁷ together with those presented in this work. Most of the (Z)- Δ Phe (**1b**) residues show average ϕ and ψ torsion angles of -62° (62°) and 21° (-21°). This clearly corresponds to the helical region, α and 3_{10} , equally right- and left-handed, although the ϕ and ψ torsion angles slightly deviate from those found for a standard amino acid. A few structures show the average ϕ and ψ torsion angles of -59° (59°) and 139° (-139°), which refer to the collagen, polyglycine II, and polyproline II helices, both left- and right-handed. Further, the (Z)- Δ Phe analogues with the chlorine atom in the phenyl ring⁶⁸ or even with 1-naphthyl⁶⁹ and 1-pyrenyl⁷⁰ in place of the phenyl ring adopt similar conformations. Therefore, the (Z)- Δ Phe residue could be considered as a ‘conformational model’ characterizing such structures.

In the case of the (*E*)- Δ Phe residues (**1a** and **2a**), a scarce amount of data was found. Nevertheless, all the calculated conformers, in contrast to the Z isomer, were found in the solid state. Particularly, the extended conformation adopted in the hereinto presented structure of Ac-(*E*)- Δ Phe-NHMe should be noted, as it seems to be inaccessible for the (Z)- Δ Phe residue. The conformations of the (Z)- Δ Phe residue with the C-terminal tertiary amide bond (**2b**) correspond to the two lowest calculated conformers. Three of the four structures adopt the lowest calculated conformation. Note that two conformations belong to the (Z)- Δ Phe residue connected with proline.^{71,72} The hereinto presented (*E*)- Δ Phe (**2a**) analogue adopts the lowest of the calculated conformations. As can be seen, the presented location of the solid-state conformations is consistent with the calculations which have been carried out.

Considering only the number of conformers (Tables 1 and 2), it can be concluded that the Z isomers have greater conformational freedom than that of the *E* isomers. However, the areas around the conformers E and H of **1a** and **2a** are rather shallow, which indicates that a change of the values of the torsion angles ϕ and ψ results in a moderate change in the energy of the conformers.

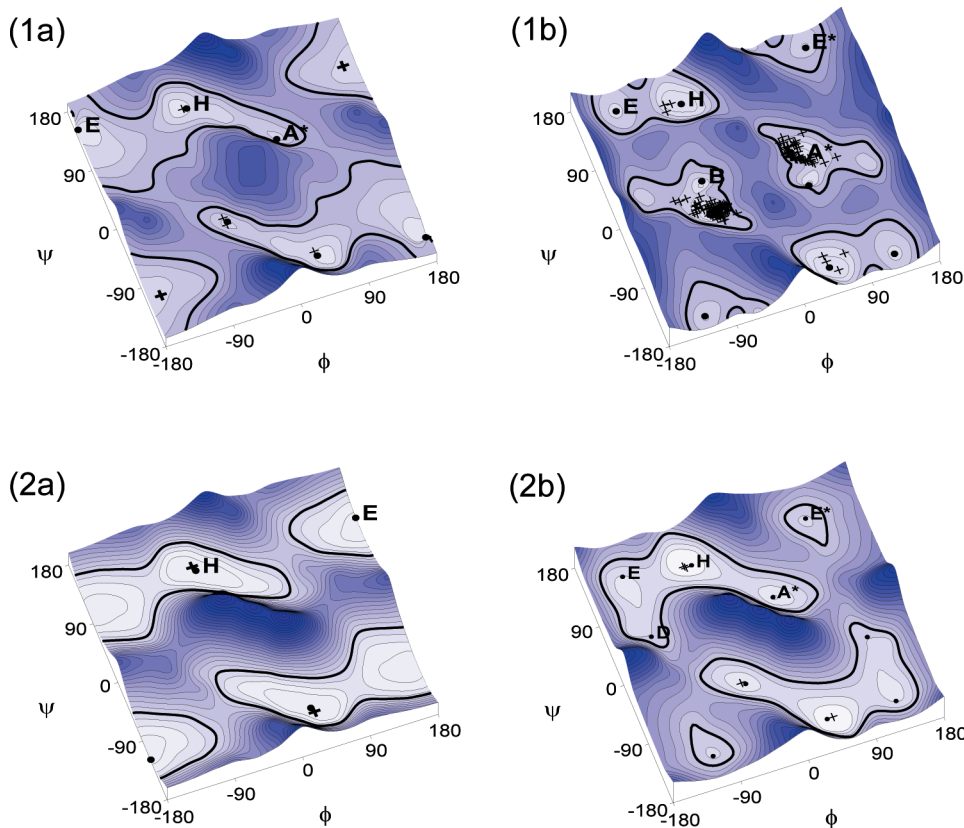


Figure 7. The ϕ , ψ potential energy surfaces of the studied molecules in a water-mimicking environment together with the solid-state conformations of analogous structures (crosses) from the Cambridge Structural Database. Bold crosses depict the solid-state conformations from the X-ray analysis presented in this work. The bold line is the energy contour 4 kcal/mol, which shows the accessible conformational space: 42% for **1a**, 37% for **2a**, 31% for **1b**, and 32% for **2b**.

Therefore, if we measure the area of the maps within the energy contour 4.0 kcal/mol, which for the theoretical method used envelops all solid-state conformations of the studied compounds, it reveals that the accessible ϕ , ψ conformational space is greater for **1a** and **2a** than for **1b** and **2b** (42%, 37%, 31%, and 32%, respectively).

CONCLUSIONS

Dehydroamino acids offer conformational properties which could be suitable for peptide design. Among dehydroamino acids, (*Z*)-dehydrophenylalanine is the one most commonly used to modify bioactive peptides because it is the most stable and relatively easy to obtain. However, there is a very little information about the conformational properties of the *E* isomer of dehydrophenylalanine. As can be seen from our study, the topography of the side chain influences the conformation of the main chain of dehydrophenylalanine both with secondary and with tertiary C-terminal amide.

The conformational preferences of two *E* isomers of dehydrophenylalanine derivatives Ac-(*E*)- Δ Phe-NHMe (**1a**) and Ac-(*E*)- Δ Phe-NMe₂ (**2a**) have been explored by X-ray diffraction at low temperature and by quantum mechanical calculations at the MP2/6-31+G(d,p) level in the gas phase and by the B3LYP/6-31+G(d,p) method in the gas phase and in a solvent environment and compared with the analogous data for the *Z* isomers (**1b** and **2b**). The results allow us to draw the following

conclusions about the conformation of these dehydrophenylalanine derivatives:

- (i) Both the *Z* and *E* isomers of Δ Phe are able to adopt conformation H and H* (ϕ , $\psi \approx \mp 40^\circ, \pm 120^\circ$) which occur in the Ramachandran map region with high energy for common amino acid residues. The conformer H is, so far, the only molecular structure that has been found in the crystal structures of Ac- Δ Xaa-NMe₂, regardless of intermolecular contacts.
- (ii) There are no helical conformers on the PESs calculated in the gas phase for the *Z* isomers of the Δ Phe residue. In the presence of a polar solvent these isomers are found to adopt the 3_{10} -helical conformation (ϕ , $\psi = \pm 67^\circ, \pm 18^\circ$ for Ac-(*Z*)- Δ Phe-NHMe and ϕ , $\psi = \pm 37^\circ, \pm 53^\circ$ for Ac-(*Z*)- Δ Phe-NMe₂). In a water environment, this conformer becomes the global minimum for Ac-(*Z*)- Δ Phe-NHMe and is the second in energy order for Ac-(*Z*)- Δ Phe-NMe₂.
- (iii) Helical conformation is not accessible for Ac-(*E*)- Δ Phe-NHMe and is highest in energy among Ac-(*E*)- Δ Phe-NHMe conformers. These *E* isomers have an intrinsic inclination to an extended conformation.

ASSOCIATED CONTENT

S Supporting Information. A figure comparing two methods of labeling backbone conformers of amino acid diamides according to their locations on a Ramachandran map; a figure

with all conformers of Ac-(Z)- Δ Phe-NMe₂; tables with selected torsion angles and the hydrogen-bond geometries for studied molecules; structural parameters for the internal H-bond and dipole interactions. This material is available free of charge via the Internet at <http://pubs.acs.org>.

AUTHOR INFORMATION

Corresponding Author

*Tel: (+48) 77 452 7111; fax: (+48) 77 452 7101; e-mail: Malgorzata.Broda@uni.opole.pl.

ACKNOWLEDGMENT

The authors gratefully acknowledge the Academic Computer Centre CYFRONET AGH of Kraków for grant MEiN/SGI3700/UOpolski/063/2006. Aneta Buczek is the recipient of a Ph.D. fellowship from a project funded by the European Social Fund.

REFERENCES

- (1) Rink, R.; Wierenga, J.; Kuipers, A.; Kluskens, L. D.; Driessens, A. J. M.; Kuipers, O. P. *Appl. Environ. Microb.* **2007**, *73*, 1792–1796.
- (2) Chatterjee, C.; Paul, M.; Xie, L.; van der Donk, W. A. *Chem. Rev.* **2005**, *105*, 633–683.
- (3) Loiseau, N.; Cavelier, F.; Noel, J.-P.; Gomis, J.-M. *J. Pept. Sci.* **2002**, *8*, 335–346.
- (4) Malbrouck, C.; Kestemont, P. *Environ. Toxicol. Chem.* **2006**, *25*, 72–86.
- (5) Herfindal, L.; Selheim, F. *Mini-Rev. Med. Chem.* **2006**, *6*, 279–285.
- (6) Namikoshi, M.; Choi, B. W.; Sun, F.; Rinehart, K. L.; Carmichael, W. W.; Evans, W. R.; Beasley, V. R. *J. Org. Chem.* **1995**, *60*, 3671–3679.
- (7) Codd, G. A.; Morrison, L. F.; Metcalf, J. S. *Toxicol. Appl. Pharmacol.* **2005**, *203*, 264–272.
- (8) Parkhurst, J. R.; Hodgins, D. S. *Arch. Biochem. Biophys.* **1972**, *152*, 597–605.
- (9) Wickner, R. B. *J. Biol. Chem.* **1969**, *244*, 6550–6552.
- (10) Bonauer, C.; Walenzyk, T.; Konig, B. *Synthesis* **2006**, 1–20.
- (11) Coulston, N. J.; Jeffery, E. L.; Wells, R. P. K.; McMorn, P.; Wells, P. B.; Wilcock, D. J.; Hutchings, G. J. *J. Catal.* **2006**, *243*, 360–367.
- (12) Nagel, U.; Albrecht, J. *Top. Catal.* **1998**, *5*, 3–23.
- (13) Abreu, A. S.; Castanheira, E. M. S.; Ferreira, P. M. T.; Monteiro, L. S.; Pereira, G.; Queiroz, M.-J. R. P. *Eur. J. Org. Chem.* **2008**, *5697*–5703.
- (14) Queiroz, M.-J. R. P.; Abreu, A. S.; Carvalho, M. S. D.; Ferreira, P. M. T.; Nazareth, N.; Nascimento, M. S.-J. *Bioorg. Med. Chem.* **2008**, *16*, 5584–5589.
- (15) Mishra, A.; Panda, J. J.; Basu, A.; Chauhan, V. S. *Langmuir* **2008**, *24*, 4571–4576.
- (16) Gupta, M.; Bagaria, A.; Mishra, A.; Mathur, P.; Basu, A.; Ramakumar, S.; Chauhan, V. S. *Adv. Mater.* **2007**, *19*, 858–861.
- (17) Świątek-Kozłowska, J.; Brasuń, J.; Chruściński, L.; Chruścińska, E.; Makowski, M.; Kozłowski, H. *New J. Chem.* **2000**, *24*, 893–896.
- (18) Ferreira, P. M.; Monteiro, L. S.; Coban, T.; Suzen, S. J. *Enzyme Inhib. Med. Chem.* **2009**, *24*, 967–971.
- (19) Mathur, P.; Ramakumar, S.; Chauhan, V. S. *Biopolymers* **2004**, *76*, 150–161.
- (20) Pietrzyński, G.; Rzeszotarska, B. *Pol. J. Chem.* **1995**, *69*, 1595–1614 and references cited therein.
- (21) Singh, T. P.; Kaur, P. *Prog. Biophys. Mol. Biol.* **1997**, *66*, 141–165 and references cited therein.
- (22) Jain, R.; Chauhan, V. S. *Biopolymers* **1996**, *40*, 105–119.
- (23) Nitz, T. J.; Shimohigashi, Y.; Costa, T.; Chen, H.-Ch.; Stammer, Ch. H. *Int. J. Pept. Protein Res.* **1986**, *27*, 522–529.
- (24) Mosberg, H. I.; Dua, R. K.; Pogozheva, I. D.; Lomize, A. L. *Biopolymers* **1996**, *39*, 287–296.
- (25) Ward, D. E.; Vazquez, A.; Pedras, M. S. C. *J. Org. Chem.* **1996**, *61*, 8008–8009.
- (26) Latajka, R.; Makowski, M.; Jewgiński, M.; Pawełczak, M.; Koroniak, H.; Kafarski, P. *New J. Chem.* **2006**, *30*, 1009–1018.
- (27) Thormann, M.; Hofmann, H.-J. *J. Mol. Struct. (THEOCHEM)* **1998**, *431*, 79–96.
- (28) Broda, M. A.; Rzeszotarska, B.; Smełka, L.; Pietrzyński, G. *J. Pept. Res.* **1998**, *52*, 72–79.
- (29) Broda, M. A.; Siodłak, D.; Rzeszotarska, B. *J. Pept. Sci.* **2005**, *11*, 235–244.
- (30) Ejsmont, K.; Makowski, M.; Zaleski, J. *Acta Crystallogr., Sect. C: Cryst. Struct. Commun.* **2001**, *57*, 205–207.
- (31) Padyana, A. K.; Ramakumar, S.; Mathur, P.; Jagannathan, N. R.; Chauhan, V. S. *J. Pept. Sci.* **2003**, *9*, 54–63.
- (32) Ramagopal, U. A.; Ramakumar, S.; Mathur, P.; Joshi, R. M.; Chauhan, V. S. *Protein Eng.* **2002**, *15*, 331–335.
- (33) Makowski, M.; Lisowski, M.; Mikołajczyk, I.; Lis, T. *Acta Crystallogr., Sect. E: Struct. Rep. Online* **2007**, *63*, o19–o21.
- (34) Makowski, M.; Lisowski, M.; Maciąg, A.; Lis, T. *Acta Crystallogr., Sect. E: Struct. Rep. Online* **2006**, *62*, o807–o810.
- (35) Makowski, M.; Brzuszakiewicz, A.; Lisowski, M.; Lis, T. *Acta Crystallogr., Sect. C: Cryst. Struct. Commun.* **2005**, *61*, o424–o426.
- (36) Chatterjee, J.; Gilon, C.; Hoffman, A.; Kessler, H. *Acc. Chem. Res.* **2008**, *41*, 1331–1342.
- (37) Kokkoni, N.; Stott, K.; Amijee, H.; Mason, J. M.; Doig, A. J. *Biochemistry* **2006**, *45*, 9906–9918.
- (38) Fulton, N. D.; Bollenbacher, K.; Templeton, G. E. *Phytopathology* **1965**, *55*, 49–51.
- (39) Rinehart, K. L.; Harada, K.-I.; Namikoshi, M.; Chen, C.; Harvis, C. A.; Munro, M. H. G.; Blunt, J. W.; Mulligan, P. E.; Beasley, V. R. *J. Am. Chem. Soc.* **1988**, *110*, 8557–8558.
- (40) Miyamae, A.; Fujioka, M.; Koda, S.; Morimoto, Y. *J. Chem. Soc., Perkin Trans. 1* **1989**, 873–878.
- (41) Takasaki, J.; Saito, T.; Taniguchi, M.; Kawasaki, T.; Moritani, Y.; Hayashi, K.; Kobori, M. *J. Biol. Chem.* **2004**, *279*, 47438–47445.
- (42) Yoshinari, T.; Okada, H.; Yamada, A.; Uemura, D.; Oka, H.; Suda, H.; Okura, A. *Jpn. J. Cancer Res.* **1994**, *85*, 550–555.
- (43) Teshima, T.; Nishikawa, M.; Kubota, I.; Shiba, T.; Iwai, Y.; Omura, S. *Tetrahedron Lett.* **1988**, *29*, 1963–1966.
- (44) Liebermann, B.; Ellinger, R.; Pinet, E. *Phytochemistry* **1996**, *42*, 1537–1540.
- (45) Broda, M. A.; Siodłak, D.; Rzeszotarska, B. *J. Pept. Sci.* **2005**, *11*, 546–555.
- (46) Siodłak, D.; Broda, M. A.; Rzeszotarska, B. *J. Mol. Struct. (THEOCHEM)* **2004**, *668*, 75–85.
- (47) Herbst, R. M.; Shemin, D. *Org. Syntheses*; Wiley: New York, 1943; Coll. Vol. 2, pp 1–3. Wong, H. N. C.; Xu, Z. L.; Chang, H. M.; Lee, C. M. *Synthesis* **1992**, 793–797.
- (48) Siodłak, D.; Broda, M. A.; Rzeszotarska, B.; Dybała, I.; Kozioł, A. E. *J. Pept. Sci.* **2003**, *9*, 64–74.
- (49) Smełka, L.; Rzeszotarska, B.; Broda, M. A.; Kubica, Z. *Org. Prep. Proc. Int.* **1997**, *29*, 696–701.
- (50) Still, W. C.; Kachn, M.; Mitra, A. *J. Org. Chem.* **1978**, *43*, 2923–2925.
- (51) CrysAlis CCD (ver. 1.171.29.10) and CrysAlis Pro (ver. 1.171.33.32); Oxford Diffraction Ltd.: Abingdon, England, 2006 and 2009.
- (52) Sheldrick, G. M. *Acta Crystallogr., Sect. A: Found. Crystallogr.* **2008**, *64*, 112–122.
- (53) Macrae, C. F.; Bruno, I. J.; Chisholm, J. A.; Edgington, P. R.; McCabe, P.; Pidcock, E.; Rodriguez-Monge, L.; Taylor, R.; van de Streek, J.; Wood, P. A. *J. Appl. Crystallogr.* **2008**, *41*, 466–470.
- (54) Frisch, M. J.; Trucks, G. W.; Schlegel, H. B.; Scuseria, G. E.; Robb, M. A.; Cheeseman, J. R.; Scalmani, G.; Barone, V.; Mennucci, B.; Petersson, G. A.; Nakatsuji, H.; Caricato, M.; Li, X.; Hratchian, H. P.; Izmaylov, A. F.; Bloino, J.; Zheng, G.; Sonnenberg, J. L.; Hada, M.; Ehara, M.; Toyota, K.; Fukuda, R.; Hasegawa, J.; Ishida, M.; Nakajima, T.; Honda, Y.; Kitao, O.; Nakai, H.; Vreven, T.; Montgomery, Jr., J. A.;

Peralta, J. E.; Ogliaro, F.; Bearpark, M.; Heyd, J. J.; Brothers, E.; Kudin, K. N.; Staroverov, V. N.; Kobayashi, R.; Normand, J.; Raghavachari, K.; Rendell, A.; Burant, J. C.; Iyengar, S. S.; Tomasi, J.; Cossi, M.; Rega, N.; Millam, M. J.; Klene, M.; Knox, J. E.; Cross, J. B.; Bakken, V.; Adamo, C.; Jaramillo, J.; Gomperts, R.; Stratmann, R. E.; Yazyev, O.; Austin, A. J.; Cammi, R.; Pomelli, C.; Ochterski, J. W.; Martin, R. L.; Morokuma, K.; Zakrzewski, V. G.; Voth, G. A.; Salvador, P.; Dannenberg, J. J.; Dapprich, S.; Daniels, A. D.; Farkas, Ö.; Foresman, J. B.; Ortiz, J. V.; Cioslowski, J.; Fox, D. J. *Gaussian 09, Revision A.02*, Gaussian, Inc.: Wallingford, CT, 2009.

- (55) Becke, A. D. *J. Chem. Phys.* **1993**, *98*, 5648–5652.
(56) Lee, C.; Yang, W.; Parr, R. G. *Phys. Rev. B* **1988**, *37*, 785–789.
(57) Miertus, S.; Tomasi, J. *Chem. Phys.* **1982**, *65*, 239–245.
(58) Tomasi, J.; Mennucci, B.; Cammi, R. *Chem. Rev.* **2005**, *105*, 2999–3093.
(59) *Surfer 8*, Golden Software, Inc., 2002.
(60) Scott, A. P.; Radom, L. *J. Phys. Chem.* **1996**, *100*, 16502–16513.
(61) Zimmerman, S. S.; Pottle, M. S.; Némethy, G.; Scheraga, H. A. *Macromolecules* **1977**, *10*, 1–9.
(62) Siodłak, D.; Broda, M. A.; Rzeszotarska, B.; Dybała, I.; Kozioł, A. E. *J. Pept. Sci.* **2003**, *9*, 64–74.
(63) Souhassou, M.; Lecomte, C.; Ghermani, N.-E.; Rohmer, M. M.; Wiest, R.; Benard, M.; Blessing, R. H. *J. Am. Chem. Soc.* **1992**, *114*, 2371–2382.
(64) Allen, F. H.; Baalham, C. A.; Lommersse, J. P. M.; Raithby, P. R. *Acta Crystallogr., Sect. B: Struct. Crystallogr. Cryst. Chem.* **1998**, *B54*, 320–329.
(65) Steiner, T. *Angew. Chem., Int. Ed.* **2002**, *41*, 48–76.
(66) Crisma, M.; Formaggio, F.; Toniolo, C.; Yoshikawa, T.; Wakamiya, T. *J. Am. Chem. Soc.* **1999**, *121*, 3272–3278.
(67) Allen, F. H. *Acta Crystallogr., Sect. B: Struct. Crystallogr. Cryst. Chem.* **2002**, *B58*, 380–388.
(68) Wen, L.-R.; Liu, P.; Li, M. *Acta Crystallogr., Sect. E: Struct. Rep. Online* **2007**, *63*, 1212–1214.
(69) Inai, Y.; Oshikawa, T.; Yamashita, M.; Hirabayashi, T.; Hirako, T. *Biopolymers* **2001**, *58*, 9–19.
(70) Inai, Y.; Oshikawa, T.; Yamashita, M.; Hirabayashi, T.; Kurokawa, Y. *Bull. Chem. Soc. Jpn.* **2001**, *74*, 959–966.
(71) Ajo, D.; Busetti, V.; Granozzi, G. *Tetrahedron* **1982**, *38*, 3329–3334.
(72) Busetti, V.; Crisma, M.; Toniolo, C.; Salvadori, S.; Balboni, G. *Int. J. Biol. Macromol.* **1992**, *14*, 23–28.